

3D RECONSTRUCTION FROM LOG-COMPRESSED RAYLEIGH IMAGES

João M. Sanches Jorge S. Marques

Instituto Superior Técnico/Instituto de Sistemas e Robótica
 Av. Rovisco Pais 1049-001 Lisboa, Portugal
 jmrs@alfa.ist.utl.pt jsm@isr.ist.utl.pt

ABSTRACT

This paper addresses 3D reconstruction in the presence of multiplicative noise and non-linear compression of the ultrasound data. Ultrasound images are often considered as being corrupted by multiplicative noise with Rayleigh distribution. However, commercial ultrasound equipment also performs a non-linear image compression which reduces the dynamic range of the ultrasound signal, for visualization purposes. In this paper the non-linear compression is explicitly modelled and considered for 3D reconstruction of medical data. The proposed algorithm is tested with synthetic and real data and the results are discussed in the paper.

1. INTRODUCTION

Three dimensional ultrasound aims to reconstruct data in a region of interest from a set of ultrasound images. Several difficulties are usually involved in this process: i) ultrasound images have a low signal to noise ratio being corrupted by multiplicative noise; ii) only a subset of the region of interest is intersected by the inspection planes requiring the use of interpolation techniques; iii) the ultrasound equipment introduces a nonlinear compression of the images which distorts the probability distribution of the observed data. Two approaches are adopted in practice to circumvent these difficulties. Simple reconstruction methods based on ad hoc procedures are sometimes used (e.g., see [1]). The main advantage of these methods lies on their ability to produce reconstruction results in real time. Other authors prefer to work with the backscattered echo (RF signal) i.e., the sensor output before being compressed (see [2, 3]). This avoids the problem of dealing with the nonlinear compression performed by the ultrasound equipment which is usually unknown. However, this approach is not always easy to implement in practice since the RF output is not available in most ultrasound equipments. The effect of non-linear pre-processing has been considered in the past, in the scope of noise reduction with median and adaptive filtering [4, 5].

In this paper the reconstruction of a 3D data volume from noisy and compressed ultrasound images is addressed. The set up is shown in Fig. 1. A free hand ultrasound probe is used to obtain a sequence of ultrasound images, corresponding to cross sections of the organ to be inspected. A spatial locator is used to measure the position of the ultrasound probe at each instant of time. Each image is

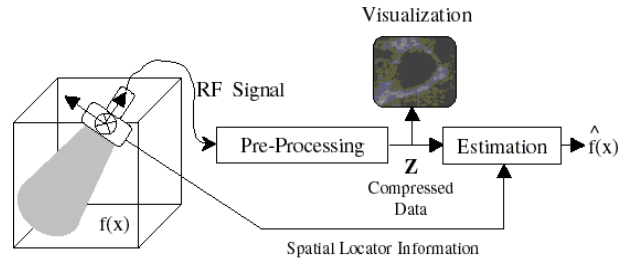


Fig. 1. Block diagram of the processing system

then pre-processed by the ultrasound equipment. Only the output of the pre-processing stage is usually available.

A Bayesian approach is adopted in this paper to reconstruct the unknown volume taking into account the multiplicative noise present in the backscattered signal, as well as the non linear compression performed by the acquisition system. Since the compression law is unknown it also has to be estimated from the observed data. The paper is organized as follows. Section 2 describes a basic reconstruction algorithm without non linearity compensation. Section 3 extends these results to encompass the compression effects. Experimental results are described in section 4 and section 5 concludes the paper.

2. 3D RECONSTRUCTION

The Rayleigh reconstruction algorithm (without non-linearity compensation) is described in [6] and will be briefly summarized here, for the sake of completeness. Consider the experimental setup described in Fig.1. Given a set of ultrasound images and the output of the spatial locator, we wish to estimate the acoustic reflectivity in a given volume of interest.

Let $U = \{u_g\}$ be a set of unknown parameters defining a 3D function f in a region of interest and let $X = \{x_i\}, Y = \{y_i\}$ denote the observed data: pixel locations in 3D space and intensities. The MAP estimate of U is obtained by minimizing

$$E = E_y + E_u \quad (1)$$

where $E_y = -\log p(Y/U)$ is minus the log-likelihood function and $E_u = -\log p(U)$ is a quadratic regularization term.

$$E_u = \psi \sum_g \sum_{j=1}^3 (u_g - u_{g,j})^2 \quad (2)$$

this work was partially supported by FCT

where u_g is a volume coefficient and u_{gj} denotes the j -th neighbor of u_g (see the details in [6]). The ψ parameter measures the strength of the connections among neighboring nodes. A high value of ψ corresponds to strongly connected neighbors (differences receive a high penalty) while low values of ψ correspond to weak connections.

It is assumed that Y is a set of i.i.d. (independent and identically distributed) random variables with Rayleigh distribution [7],

$$p(y_i/U) = \frac{y_i}{f(x_i)} e^{-\frac{y_i^2}{2f(x_i)}} \quad (3)$$

where y_i denotes the amplitude of i -th pixel of the non-compressed image sequence and $f(x_i)$ represents the reflectivity associated to the position x_i , to be estimated. It is assumed that

$$f(x) = \sum_p u_p b_p(x) \quad (4)$$

where b_p are known basis functions. Using (3), the data energy becomes

$$E_y = - \sum_i \left\{ \log\left(\frac{y_i}{f(x_i)}\right) - \frac{y_i^2}{2f(x_i)} \right\} \quad (5)$$

The minimization of (1) is performed by the ICM algorithm (see the details in [6]).

3. RECONSTRUCTION WITH COMPRESSED DATA

Unfortunately, the echo intensities Y are not available in most ultrasound equipments. Only a nonlinear version of Y is available. Here, it is assumed that the backscattered signal, Y , is modified by a non linear transformation

$$z_i = \alpha \log(y_i + 1) + \beta \quad (6)$$

where z_i is the intensity of the i th pixel and (α, β) are the unknown parameters of the compression law to be estimated. The distribution of z_i is no longer Rayleigh, being defined by

$$p(z_i) = \left| \frac{dy}{dz} \right| p(y_i) \quad (7)$$

where $p(y)$ is the density function of the original ultrasound image (Rayleigh) and dy/dz is the derivative of the inverse compression function. Using (3,7) leads to

$$p(z_i/U) = \frac{w_i(w_i + 1)}{\alpha f(x_i)} e^{-\frac{w_i^2}{2f(x_i)}} \quad (8)$$

where

$$w_i = e^{\frac{z_i - \beta}{\alpha}} - 1 \quad (9)$$

Using (8) the energy of the compressed data becomes

$$E_z = - \sum_i \left\{ \log\left(\frac{w_i(w_i + 1)}{f(x_i)\alpha}\right) - \frac{w_i^2}{2f(x_i)} \right\} \quad (10)$$

Therefore, the estimation of the U, α, β is performed by minimizing (1), after replacing E_y by E_z . The minimization of E will be split into two alternating steps (see Fig. 2): volume reconstruction and non-linearity estimation.

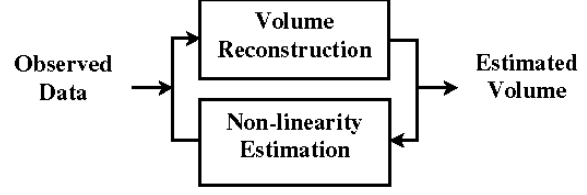


Fig. 2. Block diagram of the reconstruction process.

3.1. Volume Reconstruction

In this paper, each component u_p of U is sequentially updated by the ICM algorithm. In each iteration all the unknown variables are sequentially estimated considering (1) as an unidimensional function of u_p . The Newton-Rapson method is used to solve $\frac{\partial}{\partial(u_p)} E(u_p) = 0$ leading to

$${}^{n+1}\hat{u}_p = {}^n\hat{u}_p + \lambda \frac{0.5 \sum_i \frac{w_i^2 - 2f(x_i)}{f^2(x_i)} b_p(x_i) - 2\psi N_v (u_p - \bar{u}_p)}{\sum_i \frac{w_i^2 - f(x_i)}{f^3(x_i)} b_p^2(x_i) + 2\psi N_v} \quad (11)$$

with

$$\bar{u}_p = \frac{1}{N_v} \sum_{u_g \in \delta_p} u_g \quad (12)$$

where ${}^n\hat{u}_p$ is the estimate of u_p obtained at the n -th iteration, N_v is the number of control points inside the neighborhood δ_p of the p -th grid node ($p(N_v = 6)$) and λ is a gain.

3.2. Non-linearity Estimation

To estimate (α, β) a bidimensional version of the Newton-Rapson algorithm is used, i.e.,

$$({}^{n+1}\hat{\alpha}, {}^{n+1}\hat{\beta}) = ({}^n\hat{\alpha}, {}^n\hat{\beta}) - \nabla E(\hat{U}, {}^n\hat{\alpha}, {}^n\hat{\beta}) H^{-1} \quad (13)$$

where $\nabla E(U, \alpha_0, \beta_0)$ is the gradient vector and H is the Hessian matrix with respect to α, β . Equation (13) can be rewritten as follows

$${}^{n+1}\hat{\alpha} = {}^n\hat{\alpha} (1 - \xi_\alpha \frac{g_\beta g_{\alpha\beta} - g_\alpha g_{\beta\beta}}{g_{\alpha\alpha} g_{\beta\beta} - g_{\alpha\beta}^2}) \quad (14)$$

$${}^{n+1}\hat{\beta} = {}^n\hat{\beta} (1 - \xi_\beta \frac{g_\alpha g_{\alpha\beta} - g_\beta g_{\alpha\alpha}}{g_{\alpha\alpha} g_{\beta\beta} - g_{\alpha\beta}^2}) \quad (15)$$

where

$$\begin{aligned} g_\alpha &= \sum_i A_i \log(w_i + 1) - 1 \\ g_{\alpha\alpha} &= \sum_i 2A_i \log(w_i + 1) + B_i \log^2(w_i + 1) - 1 \\ g_\beta &= \sum_i A_i \\ g_{\beta\beta} &= \sum_i B_i \\ g_{\alpha\beta} &= \sum_i A_i + B_i \log(w_i + 1) \end{aligned} \quad (16)$$

$$\begin{aligned} A_i &= \frac{w_i^3 + w_i^2 - 2f(x_i)w_i - f(x_i)}{f(x_i)w_i} \\ B_i &= \frac{2w_i^3 + w_i^2 + f(x_i)}{f(x_i)w_i^2} (w_i + 1) \end{aligned}$$

and ξ_α, ξ_β are update gains.

It should be stressed that the estimation of α, β requires an estimate of the volume coefficients, \hat{U} . The converse

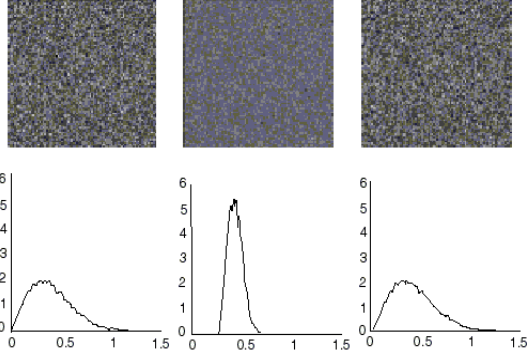


Fig. 3. Restoration results: Images and Histograms. a) Unobserved data (Rayleigh), b) Observed (compressed), c) Decompressed result

is also true. Volume reconstruction assumes that α, β estimates are available. Improved α, β estimates will allow to achieve improved volume reconstruction and vice-versa. This suggests a recursive procedure in which both steps alternate.

4. EXPERIMENTAL RESULTS

This section presents reconstruction results with synthetic and real data. Two methods are considered: i) the Bayesian reconstruction algorithm without nonlinearity compensation, and ii) the reconstruction with compensation. Three problems are considered in this section: i) the reconstruction of synthetic uniform volumes, ii) the reconstruction of synthetic non uniform volumes and iii) the reconstruction of medical data.

4.1. Uniform Volumes

Let us consider uniform volumes first i.e., $f(x) = const.$. This allows to test the performance of the proposed algorithm in the estimation of the nonlinearity parameters. An example is shown in Fig.3. Fig.3a shows a synthetic image with random Rayleigh distributed pixels. The histogram of the pixel intensity is shown below. Fig.3.b shows the log compressed image obtained by applying the non-linear transformation (6) to the pixels of the original image with $\alpha = \beta = 20$. The histogram is no longer Rayleigh as shown in the figure. Finally Fig.3.c shows the estimated image using the log compressed model. It is concluded that the estimated image is similar to the original image and their histograms are almost identical, showing the ability of the algorithm to recover the original data.

Monte Carlo tests were performed to evaluate the mean and standard deviation of $\hat{\alpha}, \hat{\beta}$ as a function of α, β . The results were obtained with 20 Monte Carlo runs. In each run, the parameters were estimated using a uniform cross section with 128×128 pixels. It was experimentally observed that the MAP estimates are unbiased and their standard deviations increase linearly with α .

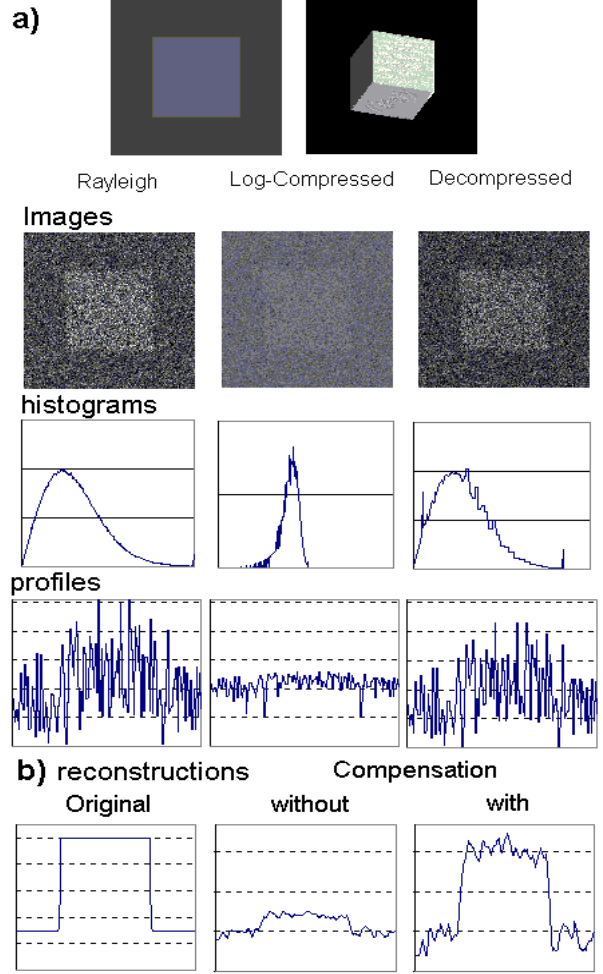


Fig. 4. Reconstruction/Restoration results using a 3D synthetic cube. Data: set of 50 cross-sections corrupted by Rayleigh noise and log-compressed with $\alpha = 20, \beta = 20$. Reconstructions methods: with and without non-linear model ($\hat{\alpha} = 20.5, \hat{\beta} = 19.7$).

4.2. Non Uniform Volumes

Let us now consider the reconstruction of non uniform volumes. For the sake of simplicity, it is assumed that the function $f(x)$ to be estimated is binary: it has a high value inside a cube to be reconstructed and a low value outside. Several experiments were performed. In each experiment 50 cross sections of the object are computed. The Rayleigh distributed images are compressed by the log compression law using selected values for α, β . Then, the algorithm described in this paper is used to simultaneously reconstruct the volume and estimate the α, β parameters. Fig.4.a illustrates the steps involved in one experiment and Fig.4.b shows the reconstruction results without and with compensation. Comparing the reconstructed profiles with the original one, it is observed that a significant improvement is achieved by using the non-linearity compensation. Table 1 shows the performance of both models for three different values of α . The likelihood function and the SNR are used

α	β	with comp.				without comp.	
		$\hat{\alpha}$	$\hat{\beta}$	l	SNR	l	SNR
1	0	1.0	0.0	-10.8	6.3	-27.5	-38.0
10	0	10.0	0.0	-40.7	6.3	-53.0	3.4
50	0	50.2	0.0	-61.5	6.3	-80.4	1.5

Table 1. Simulation results with synthetic data (Cube).

to evaluate the reconstruction results. This table shows a clear improvement of the log-likelihood and SNR values when the non-linearity compensation is used. The estimates of α, β parameters obtained in these experiments are close to the true ones.

The reconstruction results obtained with the non-linearity estimation, proposed in this paper, are clearly better than the ones obtained by a straight forward application of the Bayesian reconstruction algorithm. It should be stressed that the estimated volumes obtained with image compensation are almost invariant with respect to the values of α, β . Furthermore, it was observed that the nonlinearity compensation also improves the convergence of the reconstruction algorithm.

4.3. Medical Data

The proposed algorithm was used in the reconstruction of human organs using sequences of ultrasound images. Fig. 5, shows the results obtained for the reconstruction of a thyroid from a set of 100 images. Although the output of the reconstruction process is a 3D function, we preferred to visualize the intensity profiles of the reconstructed volume. Figure 5 shows four cross sections of the thyroid and the intensity profiles obtained by sampling the reconstructed volume along specific lines. To compute these profiles a transformation is needed to convert f values into image intensity values. Two different transformations were used according to the model used:

Rayleigh model without compensation

$$I(x) = \frac{2\hat{f}^2(x)}{\pi} \quad (17)$$

Rayleigh model with compensation

$$I(x) = \hat{\alpha}(\log(2\hat{f}(x)) - \gamma)/2 + \hat{\beta} \quad (18)$$

It is concluded that the algorithm presented in this paper provides a better representation of details (see Fig.5.c and Fig.5.d). Furthermore, the use of nonlinearity compensation allows a significant improvement of convergence rate.

5. CONCLUSIONS

This paper presents an algorithm to estimate the reflectivity function, $f(x)$, in a given region of interest from a set of compressed ultrasound images. A Bayesian approach is used to estimate this function, by assuming that the position and orientation of the ultrasound probe are accurately known. The log-compression process performed at the pre processing stage of the ultrasound equipment is explicitly

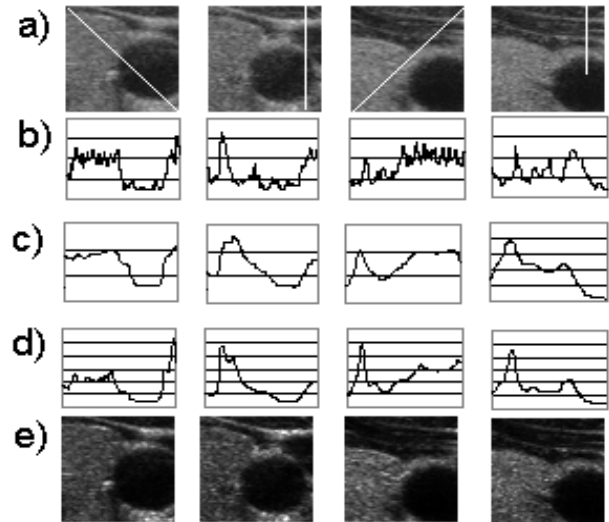


Fig. 5. Thyroid Reconstruction: a) original images, b) original intensity profiles, reconstruction results c) without and d) with non-linearity estimation, e) compensated images

considered and compensated. The estimation of the log-compression parameters is simultaneously performed with the volume reconstruction by optimizing a common objective function (posterior density of the unknowns parameters).

The proposed algorithm was evaluated with synthetic and real data. It was shown that it allows an accurate estimation of the compression law while it simultaneously improves the reconstruction results. Furthermore, it also speeds up the optimization process by improving the convergence rate.

Acknowledgment

The ultrasound data was kindly provided by J. Carr and R. Prager from the University of Cambridge.

6. REFERENCES

- [1] R.N.Rohling, et al., A comparison of freehand three-dimensional ultrasound reconstruction techniques, *Medical Image Analysis*, 339-159, 1999.
- [2] J. H. Hokland, Markov Models of Specular and Diffuse Scattering in Restoration of Medical Ultrasound Images, *IEEE TUFFC*, 660-669, July 1996.
- [3] R.M.Cramblitt, K.J.Parker, Generation of Non-Rayleigh Speckle Distribution Using Marked Regularity Models, *IEEE TUFFC*, 867-874, July 1999.
- [4] M.Karaman, M. A. Kutay, G. Bozdagi, An Adaptive Speckle Suppression Filter for Medical Ultrasonic Imaging, *IEEE TMI*, 283-292, June 1995.
- [5] V. Dutt, Adaptive Speckle Reduction Filter for Log-Compressed B-Scan Images, *IEEE TMI*, 802-813 December 1996.
- [6] J. Sanches, J. Marques, A Rayleigh reconstruction/interpolation algorithm for 3D ultrasound, *Pattern Recognition Letters*, 21, 917-926, 2000.
- [7] C. Burckhardt, Speckle in Ultrasound B-Mode Scans, *IEEE TSU*, 1-6, January 1978.